A new approach of vacuum preloading with booster PVDs to improve deep marine clay strata

Yuanqiang Cai [1], Zhiwei Xie [2], Jun Wang [3], Peng Wang [4], Xueyu Geng [5]

1. Professor, Key Laboratory of Engineering and Technology for Soft Soil Foundation and Tideland Reclamation of Zhejiang Province, Wenzhou Univ., Zhejiang 325035, P.R. China; College of Civil Engineering and Architecture, Zhejiang University of Technology, Hangzhou 310014, China; Innovation Centre of Tideland Reclamation and Ecological Protection, Wenzhou Univ., Wenzhou, Zhejiang 325035, P.R. China; Email:caiyq@zju.edu.cn

2. Master, College of Architecture and Civil Engineering, Wenzhou Univ., Wenzhou, Zhejiang 325035, P.R. China. Email: zhiweixie1963@163.com

3. Professor, College of Architecture and Civil Engineering, Wenzhou Univ., Wenzhou, Zhejiang 325035, P.R. China. Tel: +86-15968795938, Fax: +8657786689611 Email: *sunnystar1980@163.com*

4. Associate Professor, College of Architecture and Civil Engineering, Wenzhou Univ., Wenzhou, Zhejiang 325035, P.R. China. 325035, P.R. China, E-mail: geowangpeng@163.com

5. Associate Professor, School of Engineering, University of Warwick, Coventry, CV4 7AL, UK. Email: xueyu.geng@warwick.ac.uk

Abstract:

This paper presented a new approach for ground improvement of deep marine clay. In which, the conventional booster tube in the current air booster vacuum preloading technology was replaced by the booster PVD. In comparison to the ordinary PVD, the booster PVD could provide inflow channels for the compressed air when the booster pump was in operation. To examine the performance of this new air booster vacuum preloading technology, in-situ field tests were conducted at Oufei sluice project, where the thickness of the soft soil layers (i.e., marine clay) was more than 20 m. An extensive monitoring system was implemented to measure the vacuum pressure, pore water pressure, settlement, and lateral displacement at this reclamation site. With the collected field monitoring data, a comprehensive data analysis was carried out to evaluate the extent of ground improvement. The study results depicted that this new air booster vacuum preloading technology was more effective for the ground improvement of the deep marine clay layers, in comparison to the conventional vacuum preloading technology.

Author keywords: Land reclamation, Soft clayey soils, Air booster, Vacuum preloading

1 Introduction

Vacuum preloading is one of the well-established technologies for soft ground improvement. It creates negative pressure in the soil through covering the ground surface with an airtight membrane and pumping the air from the soil with prefabricated vertical drains (PVDs). Under the influence of the negative pressure, the water in the pores of the soil moves toward the surfaces via vertical drains, accompanied by a reduction in the pore water pressure and an increase in the effective stress, which thereby promotes the soil consolidation. This technology was first proposed by Kjellman (1952) to improve the subsoils properties of Philadelphia International Airport, USA. From then, a number of scholars have begun to investigate the use of vacuum preloading for the ground improvement of soft soils (Kianfar et al. 2015; Wu et al., 2015; Perera et al. 2016; Wang et al. 2016a; 2016b; 2018a; Cai et al. 2017; Fu et al. 2017; 2018; Liu et al. 2017). With these efforts, the vacuum preloading is blossoming into a popular soft ground improvement technology. Nowadays, successful implementations of vacuum preloading technology for ground improvement of the subsoil of airports, railways and highways have been widely reported around the world (e.g., Chu et al. 2000; 2004; 2005a; 2005b; 2006; Shen et al., 2005; Chai et al. 2005; 2006; 2010; Indraratna et al. 2014; Saowapakpiboon et al. 2008; Wang et al. 2017; 2018b). In the recent decades, the vacuum preloading technology has also been adopted in the land reclamation where the clay slurry dredged from seabed is used as fill material (Sun et al. 2017; Wang et al. 2016a). In that the untreated soil is oftentimes too soft for the surcharge to be applied, the vacuum preloading technology could be more attractive than the surcharge preloading technology. For example, thousands of hectares of land have been reclaimed in southeastern coastal cities in China with the vacuum preloading technology.

The other side of the coin is that the conventional vacuum preloading technology is not free of problems. 1) the blockage of the drainage channel could lead to the reduction of the drainage capacity over elapsed time, in fact, deep soil is more difficult to be further reinforced by longer drainage channels due to clogging; 2) the open style connection of the PVDs in the sand cushion might lead to the excessive dissipation of vacuum pressure, the lower vacuum pressure is not good for the consolidation of soil (Chai and Miura 1999; Bo 2004; Chai et al. 2004). To overcome these issues, an air booster vacuum preloading technology has been proposed (Shen et al. 2011; 2012; 2015; Liu et al. 2014). The idea behind this air booster vacuum preloading technology is to apply additional pressure difference between the booster tube and the PVDs, as such the dewatering and consolidation of soil in the late stage of vacuum preloading could be accelerated. In addition, there are some benefits to this technology. Firstly, the compressed air from booster system imposes a flush effect on the fine particles aggregated on the PVDs, which helps mitigate the blockage of the drainage channel and enhance the drainage capacity of the PVDs. Another advantage of this technology is the way of seal connection between tube and PVD. The seal connection of air booster vacuum preloading technology not only can reduce the loss of vacuum during the long-time operation but remove the corresponding cost of the sand cushion. Further, an extra effect of the technology can greatly shorten preloading time and improve the degree of consolidation of soil.

Verifications of the air booster vacuum preloading technology have been carried out via in-situ field tests and it has been shown that a more rapid improvement in the soils parameters could be achieved with this technology (Shen et al. 2015; Ding et al. 2015; Wang et al. 2016). It is worth noting that the booster tubes which are made of flexible brackets and filter clothes can only be inserted into a depth of 5 m with manpower and a maximum depth of 8 m with the high pressure water jet; thus, the use of the booster vacuum preloading technology in the ground improvement of deep soft soil might be limited. However, the soft clayey subsoil with a depth of 20 m could be widely encountered in practice. This potential limitation of the air booster vacuum preloading technology therefore necessitates the modification or improvement.

In this study, an improved air booster vacuum preloading technology is proposed for the ground improvement of deep marine clay. The major improvement is the dual-functional PVD (termed as booster PVD), which can be easily inserted into the deep marine clay without special equipment and efforts. Part of the booster PVD could provide an inflow channel for the compressed air when the booster pump is activated; otherwise, it plays as an ordinary PVD providing the outflow channel for the air and water. In-situ field tests were conducted to examine the performance of the improved air booster vacuum preloading technology; in which, an extensive monitoring system was implemented to measure the vacuum pressure, pore water pressure, settlement and lateral displacement. With of the field monitoring data, a comprehensive data analysis was carried out to evaluate the extent of soil improvement, and through which the significance of the improved air booster vacuum preloading technology could be demonstrated.

2 Improved air booster vacuum preloading technology

Fig. 1 illustrates the stress states of the soil element during the air booster vacuum preloading process. Initially, the soil element is in an equilibrium state under the actions of the in-situ vertical stress σ_{v0} and horizontal stress σ_{h0}, as shown in Fig. 1(a). By applying a vacuum pressure, as shown in Fig. 1(b), the soil element will be subjected to an additional isotropic incremental stress $\Delta\sigma_{vp}$. The soil element trends to consolidate under the incremental stress accompanied with the deformations of the vertical settlement and the inward lateral displacement. As the vacuum preloading proceeds, the consolidation of the soil element under the vacuum pressure fulfills gradually. Next, the booster system is activated and a booster pressure is imposed on the soil element. As shown in Fig. 1(c), the soil element further gains an incremental stress $\Delta\sigma_{bp}$ and thereby undergoes more compressive deformations, which promotes the consolidation of the soil element. During boosting process, the soil will be disturbed by booster airflow. The disturbance will destroy the micro-structure of the soil but only the disturbance will not reduce the void ratio of a soil. It is after the disturbance, the soil particles will try to reach a new steady state and the void ratio will be reduced due to "disturbances induce consolidation (Azari. et al. 2016; Yu. et al. 2009; Haeri. et al. 2016) In addition, more cracks will also generate due to the disturbance of airflow. The cracks shorten the seepage path of water in soil void, which promotes the dissipation of the water and thereby accelerates the consolidation of the soil.

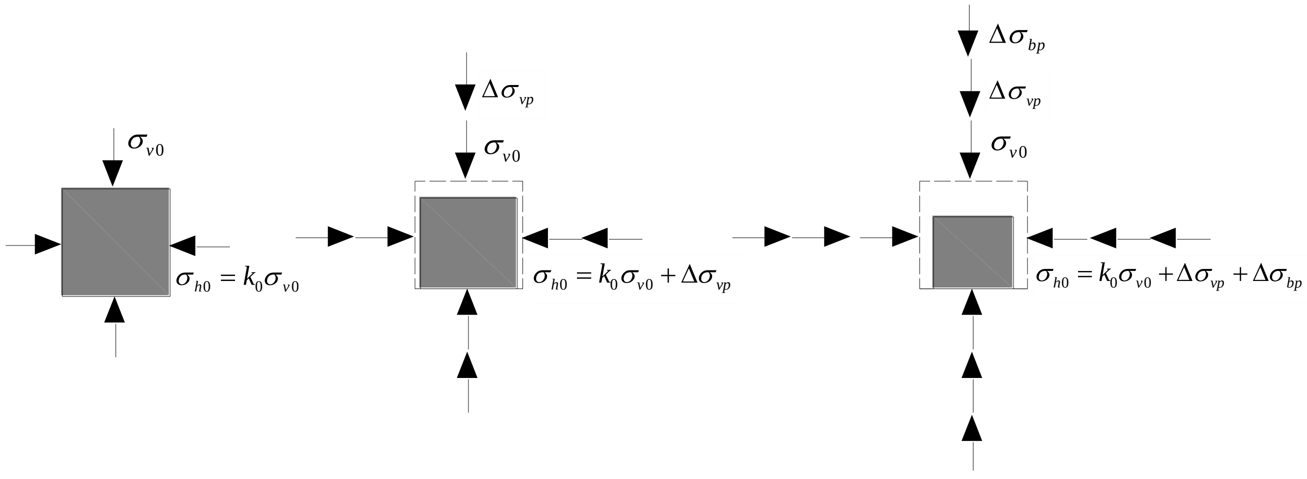

(a) (b) (c)

Fig. 1. Stress state of the soil element subjected to vacuum pressure and boost pressure: (a) initial stress state; (b) stress state under vacuum pressure; (c) stress state under vacuum pressure and booster pressure

In the later period of the consolidation, the scouring influence of airflow of booster system can effectively alleviate the problem of clogging of PVDs. In booster PVDs, the function of booster PVDs will be altered from draining to air boosting because of the activation of the booster system. The pressure difference between booster PVD and PVD will keep squeezing the soil between them to promote drainage, then the discharge water also scour the PVD to take away the fine particles of clogging. In addition, the airflow from the booster pump could wash the booster PVD's drainage channel and filter jacket directly to allow them to operate more smoothly. Meanwhile, the airflow in soil will continue to discharge through the PVDs under the vacuum pressure, and it also plays a role of wash PVD in this process. These functions directly promote the drainage capacity of PVD, and thus indirect enhance the degree of consolidation of the soil.

As mentioned above, one of the main limitations that prevent the successful implementation of the air booster vacuum preloading technology, in the site applications, is the small embedment depth of the booster tube. Fig. 2 (a) shows the picture of a booster tube which is conventionally used in the air booster vacuum preloading technology. The booster tube is composed of permeable tube segments connected in series by threaded joints, which are made of spiral flexible brackets and filter clothes. Because of the small stiffness, the booster tube can only be embedded into a maximum depth of 8 m even with the aid of the high pressure water jet. This embedment depth is certainly not sufficient for the site applications of soil reinforcement in the southeastern coastal areas of China, where the depth of the soft clay could be as large as 20 m. Note that although the PVDs in the conventional vacuum preloading technology only serve as the outflow channels of the water in the soil, they could certainly perform as the inflow channels of compressed air in the air booster vacuum preloading technology. Thus, the authors proposed the use of PVDs to replace the booster tubes such that the air booster vacuum preloading technology could be applied to the sluice site applications of soil reinforcement. By replacing the booster tubes with booster PVDs (shown in Fig 2b), the small embedment depth of the booster tube can be solved without any additional efforts, as the booster PVD can be inserted into the same depth without any additional effort comparing the ordinary PVD. Here, the booster PVD is designed with dual functions: part of the booster tube could provide the inflow channel of the compressed air when the booster pump is activated; otherwise, the booster tube only plays as an ordinary PVD, providing the outflow channel of the air and water in the soil.

(a) (b)

Fig. 2. Illustration of the booster pipeline (a) conventional tube and (b) booster PVD

Fig. 3 presents a schematic layout of the improved air booster vacuum preloading system. The PVDs are arranged in equilateral triangle grids. The PVD at the center of a hexagon acts as a booster PVD while the adjacent six PVDs serve as ordinary PVDs. The distance between the adjacent PVDs is determined by their effective radius of influence. According to the theories of the consolidation of a unit cell (Biot's. 1941; Onouse. 1988; Yoshikuni and Nakanodo. 1974; Rixner et al. 1986; Chai and Miura. 1999; Chai et al. 2011), i.e., a cylinder of soil surrounding a single vertical drain, the effective radius of influence can be estimated as

[1] $$r_e = (15 \sim 22) r_w$$

where r_e is the effective radius of influence of the unit cell; and r_w is the equivalent drain radius of a band-shaped PVD, which can be obtained as

[2] $$r_w = \frac{(a+b)}{4}$$

where a and b are the width and thickness of the PVD, respectively. With the equal area principle, the radius of the unit cell in a triangular layout can be calculated as

$$r = 0.525S \quad [3]$$

where S is the spacing between the adjacent PVDs. By setting $r_e = r$, the spacing between the adjacent PVDs can be determined. The embed depth of the PVDs is mainly dependent on the original properties of the soil as well as the demanded properties of the soil. And both the ordinary and booster PVDs are embedded into the soil with the help of spile equipment.

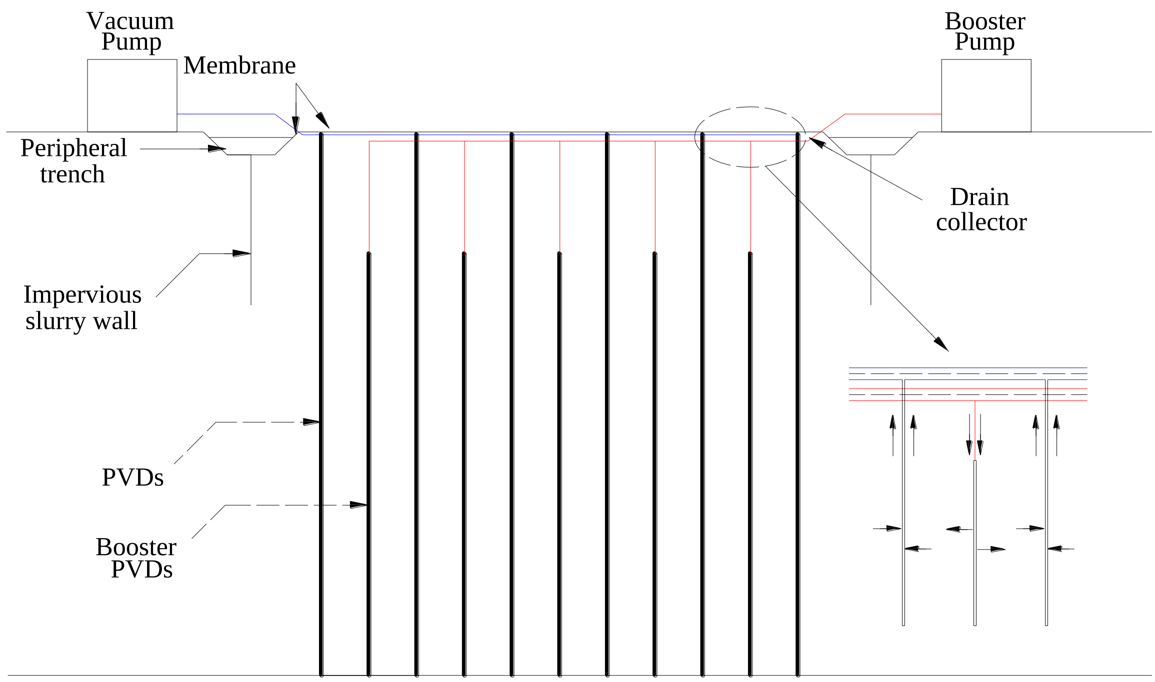

Fig. 3. Schematic layout of the improved air booster vacuum preloading system

On the ground surface, horizontal drains are placed between two adjacent rows of PVDs, which are connected with the ordinary PVDs at the two sides of the vacuum pump. In addition, horizontal booster pipes are laid out between two adjacent rows of PVDs to link the booster PVDs at the two sides to the vacuum pump or air compressor. To avoid the leakage of compressed air to the ground surface, imporous hose is employed to replace the booster PVD in the shallow soil layer (i.e., no less than 1 m). The imporous hose is linked to the booster PVD at one end of hose via hand connector and to the horizontal booster pipe at the other end via T joint. Because of the adopted airtight connections, the sand blanket which is usually laid on the ground surface in conventional vacuum preloading technology is no more required in the improved air booster vacuum preloading technology. To seal the area to be improved, two layers of geomembrane are covered on the ground surface, and the geomembrane is anchored into a trench and sealed off with a clay revetment.

3 In-situ field tests

3.1 Site conditions

To examine the performance of the improved air booster vacuum preloading technology, in-situ field tests have been carried out at Oufei sluice project in Wenzhou, China. Fig. 4 depicts the planning map of this project. It is the largest individual tideland reclamation program implemented in China, through which a total area of 323.4 km^2 from the Eastern Sea belt of China in between the estuaries of the Ou River and the Feiyun River will be reclaimed. At the testing site, a sluice gate will be built upon the completion of the ground improvement. The detailed soil profiles at both Zones A and B are presented in Fig. 5. It can be seen from Fig. 5 that the soil profile and properties at Zones A and B are differ slightly, and the marine soil is mainly composed of silt, silt clay, silty clay and muddy-silty clay. The basic soil properties, including the liquid limit (w_L), plastic limit (w_P), water content (w), specific gravity (G_s), void ratio (e_0) and vane shear strength (C_u) are summarized in Table 1. In addition, due to the poor engineering properties of marine soil at the site (high water content and high compressibility), the bearing capacity has to be improved.

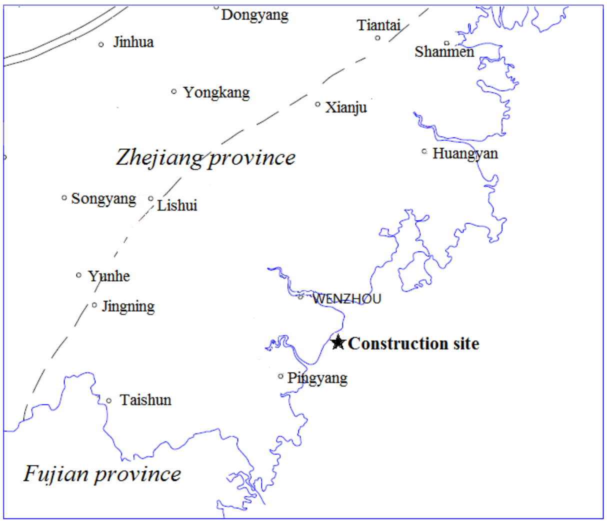

Fig. 4. Location of the test site in Wenzhou, Zhejiang province, China

Table1. Physical and mechanical properties in each soil region

Depth	Water content	Void ratio	Vane shear strength	Liquid limit	Plastic limit	Description of soil
m	%	-	kPa	%	%	-
1.4-1.7	49.6-51.5	1.44-1.85	13.67-18.5	47.1-48.6	22.4-24.3	Silt
5-5.5	55.2-58.5	1.45-1.55	18.5-19.7	42.9-48.5	22.4-24.2	Muddy-silty clay
10-10.3	47.3-53.4	1.16-1.25	23.65-25.36	38.6-41.1	21-21.9	Silt clay
15-15.3	49.9-53.4	1.55-1.56	21.56-23.25	45.2-46.4	23.1-23.5	Silt clay
20-20.3	50.8-51.1	1.62-1.69	23.3-23.88	48-48.3	24-24.1	silt

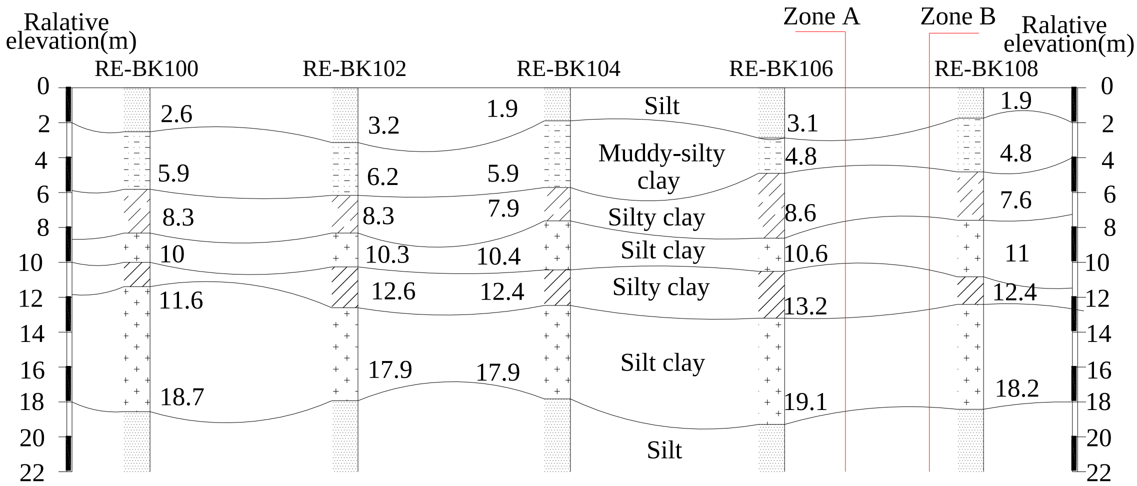

Fig. 5. Subsurface conditions for Oufei land reclamation site

3.2 Soil improvement procedure

To provide a baseline for comparison, the conventional vacuum preloading technology was also tested at the testing site; as such the testing site was divided into two zones, as shown in Fig 6. In Zone A, the conventional vacuum preloading technology was tested. In zone B, the improved air booster vacuum preloading technology was tested. The size of each zone is 40 m by 10 m, and the two zones are separated by an isolation ditch of 1.5 m deep. Because of a sluice gate will be built at the testing site after the completion of the soil improvement, and the sluice gate will subject to horizontal and vertical loads. Therefore, the requirement of depth of soil reinforcement is higher. According to relative engineering experience (Han et al. 2012; Li et al. 2011; Li et al. 2014), the depth of improved area by PVDs is determined using the influence depth of superstructure loading.

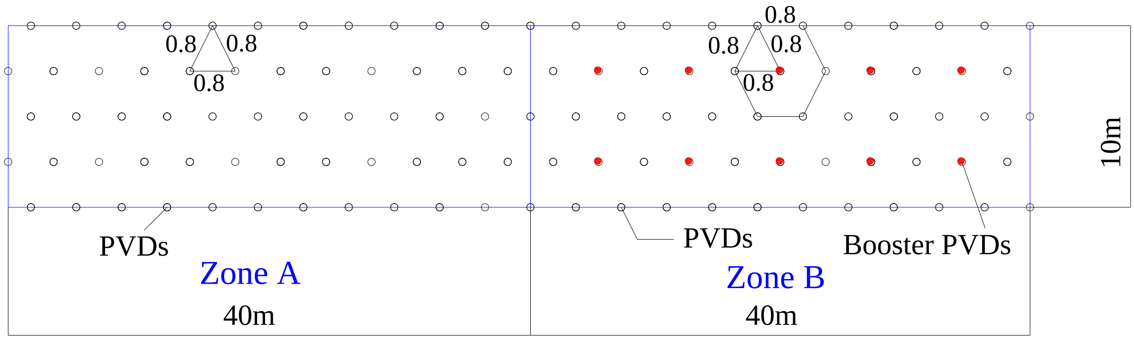

Fig. 6. Layout of in-situ test site

The implementation of the improved air booster vacuum preloading technology was elaborated as follows. Off-the-shelf PVDs were employed in this study, which were 100 mm in width and 4 mm in thickness, resulting in an equivalent drain radius of 26 mm. In reference to Eq (1) and (3), the spacing between the adjacent PVDs was estimated to fall in a range of 742-1090 mm. In order to ensure that the soil can be better reinforced, the spacing between the adjacent PVDs was determined as 800 mm. Hitherto, an improved air booster vacuum preloading system was then installed as it was prescribed in Section 2. As the marine soil was too soft to support the system installation activities, a layer of geotextile was first laid on the ground surface. Upon the completion of the air booster vacuum preloading system, the vacuum system was activated. A vacuum pressure of 85 kPa was applied and maintained using jet pumps with a power of 7.5 kW. In the first stage, the booster PVDs were connected to the jet pumps and thereby functioned as ordinary PVDs. for the first stage lasted 72 days, no notable dissipations of the pore water pressure were observed in deep layers, implying that the discharge capacity of the PVDs was greatly degraded. In the second stage, the booster system was activated through connecting the booster PVDs to the booster pump, and a positive pressure of 20 kPa was selected in this study. This positive pressure was generated by the booster pump with a power of 2.5 kW. It worked 2h/day till the end of the preloading. In addition to 2hour of booster time, the booster PVD is still used to drainage at other times. The preloading was terminated as the following two requirements were both satisfied: 1) the average settlement was less than 2 mm/day for a consecutive 5 days; and 2) the dissipation of pore pressure was less than 0.02 kPa/day for a consecutive 5 days. In this study, the preloading was terminated after 92 day.

The ground improvement procedure in zone A was similar to that in Zone B, except that the air booster system was adopted. In the conventional vacuum preloading system, the horizontal drains are formed by two kinds of pipes, that is, main pipes and branch pipes. The branch pipes were laid horizontally to link the PVDs to the main pipes, which were then connected to the jet pumps. Corrugated flexible pipes with 100 mm in diameter were used as horizontal pipes. They were perforated and wrapped with a permeable fabric textile, which served as a filter layer. To transfer the vacuum pressure to the PVDs, a layer of sand blanket with a thickness of 0.5 m was laid on the top of the horizontal drains. The test was also terminated after 92 days.

3.3 Field monitoring system

To evaluate the extent of the ground improvement, a comprehensive monitoring system was designed to record the vacuum pressure, pore water pressure, settlement, and lateral displacement. Fig. 7 shows the layout of the monitoring system. In each zone, two sets of syringe needles were employed to monitor the vacuum pressure in the PVDs. Three syringe needles were equally distributed in the upper 2 m of the

PVDs in each set. Four pore water pressure transducers were installed for the monitoring the pore water pressure at the depth of 5, 10, 15 and 20 m, respectively. A multi-level settlement gauge was utilized to record the layered settlement; and two settlement plates were used to measure the surface settlement. One inclinometer was placed at each side of the zone for monitoring the lateral displacement. In addition, field vane shear tests and cone penetration tests were performed before and after the ground improvement. Soil samples within a radial distance of 10 cm to 30 cm from the PVDs were collected for the laboratory tests.

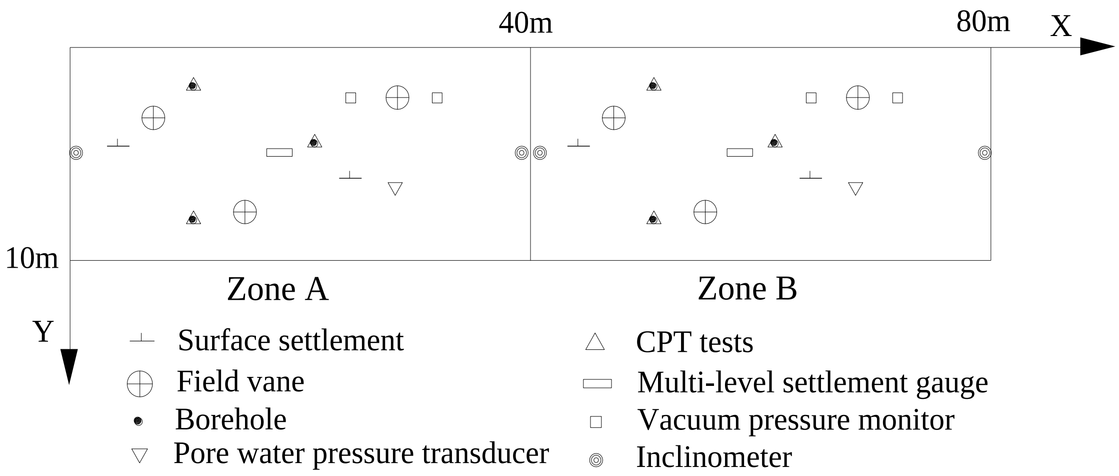

(a) Plan view

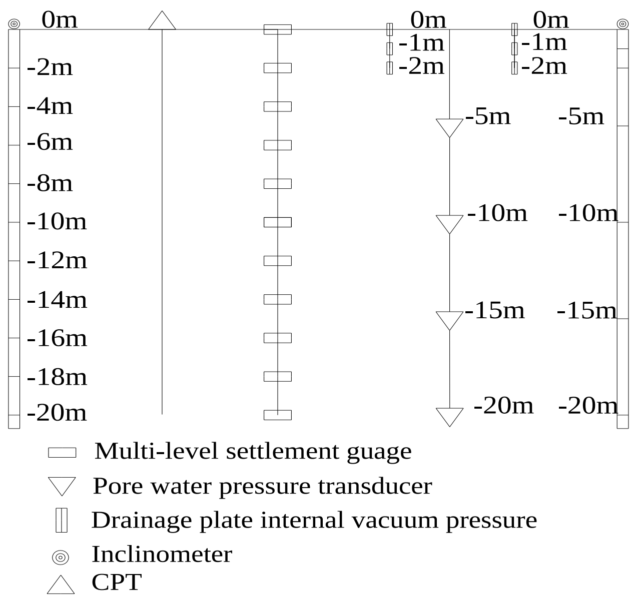

(b) Elevation view

Fig. 7. Layout of the installed instruments: (a) Plan view and (b) Elevation view

4 Results and discussions

4.1 Vacuum pressure

Fig. 8 shows the distribution of vacuum pressure in the PVDs for the two zones. In Zone A, where the conventional vacuum preloading technology was implemented, notable decrease in the vacuum pressure was observed along the depth and the vacuum loss was much more apparent in the shallow layer, as shown in Fig. 8(a). For example, the vacuum gradient was 15 kPa/m in the upper 1 m, whereas the vacuum gradient was about 8 kPa/m in the depth of 1 m to 2 m. This observation might be attributed to the poor vacuum transmission of the sand blanket covered on the ground surface. Throughout the test, the vacuum pressure remained almost stable and only small fluctuations could be identified at each individual depth.

In Zone B, where the improved air booster vacuum preloading technology was implemented, the decrease in the vacuum pressure along the depth was also observed, as shown in Fig. 8(b). Because of the airtight connections adopted in the improved air booster vacuum preloading technology, the vacuum loss along the depth was smaller in Zone B. For example, the average vacuum pressure over the first 72 days (without booster system) was 82 kPa at the depth of 2 m in Zone B, whereas that was only 72 kPa in Zone A. Further the vacuum loss along the depth was more uniform in Zone B. For example, the vacuum gradient was 6 kPa/m in average in the upper 2 m. The vacuum pressure in Zone B maintained stable before the activation of the booster system; however, this vacuum pressure experienced large fluctuations when the booster system was activated. Fig. 8(c) shows the change of vacuum pressure during boosting on the first day of the activation of the booster system. Once the booster system was activated, the vacuum pressure dropped quickly in the first 1.5 hours; after that, the vacuum pressur tended to be stable with small fluctuations. As such, the booster system was turned off after 2 hours. Upon the shutdown of the booster system, the vacuum pressure recovered rapidly to the state before the pressurization within half an hour.

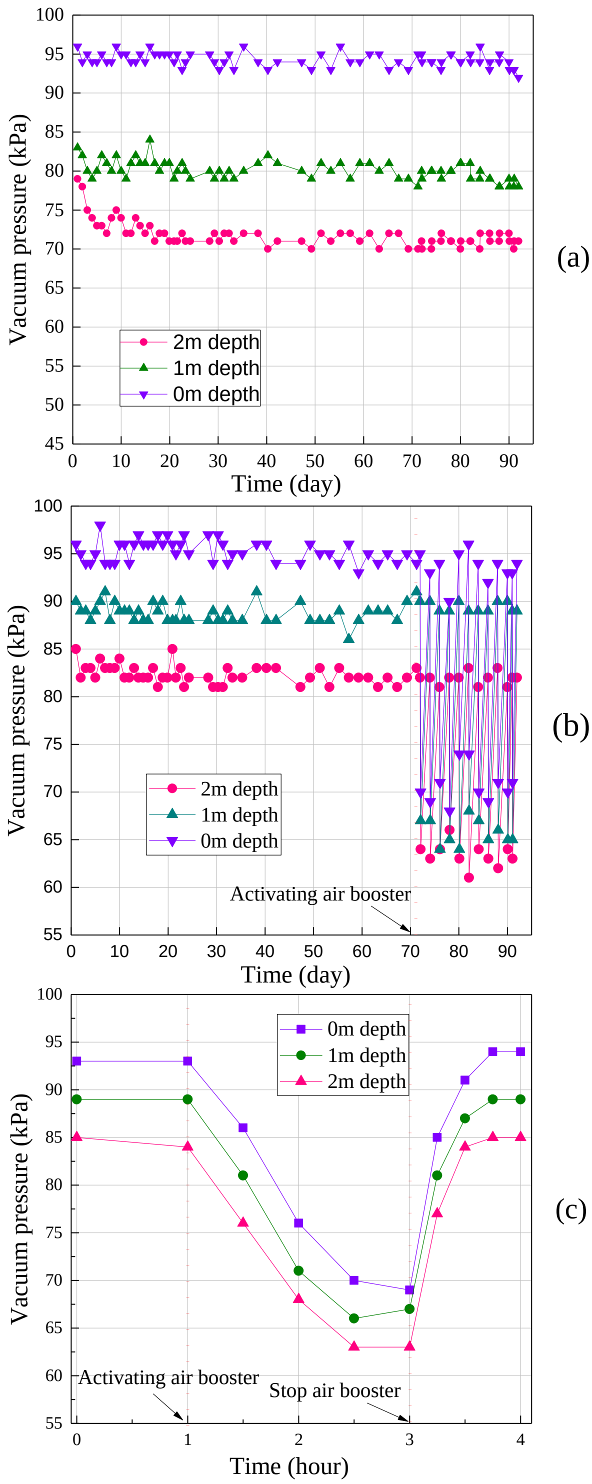

Fig. 8. Variations in the vacuum pressure in PVDs: (a) in zone A; (b) in zone B; (c) on the first day of the activation of the booster system in zone B

4.2 Pore water pressure

Fig. 9 shows the distribution of the monitored pore water pressure in the soil for the two zones. The plots in Fig. 9(a) show a rapid dissipation of the pore water pressure at the beginning of the preloading in Zone A. For example, the pore water pressure was dropped by 32.6 kPa, 28 kPa, 19.8kPa and 15.2kPa at the depth of 5 m, 10m, 15m and 20m, respectively, in the first 20 days, accounting for 63%, 67%, 61% and 37% of the total pore water pressure dissipated at the end of the preloading. Because of the vacuum loss along the depth, the dissipation rate of the pore water pressure decreased along the depth in the early stage. As the test proceeded, the dissipation of pore water pressure slowed down gradually and the difference in the dissipation rate along the depth became negligible. After 72 days of preloading, the dissipation rate of the pore water pressure decreased to less than 0.05 kPa/day at all depths. At the end of the test, the pore water pressure was decreased by 51.4 kPa, 41.7 kPa, 32.4 kPa and 41.2 kPa at the depth of 5m, 10m, 15m and 20m, respectively. It is noted that the dissipation of pore water pressure at the depth of 20 m is larger than the counterpart at the depth of 15 m, which might be interpreted by the following fact: the silt clay at the depth of 15 m causes more severe congestion in the PVDs than the silt at the depth of 20 m.

The dissipation of the pore water pressure in Zone B was similar to that in Zone A before the activation of the booster system, as shown in Fig. 9(b). Because of the larger vacuum pressure induced by the airtight connection technology, the dissipation of pore water pressure in Zone B was much faster in the early stage of this test. After 72 days’ of preloading, the difference between the pore water pressures in the two zones accumulated up to 23.1 kPa, 23.0 kPa, 19.0 kPa and 15.4 kPa at the depth of 5 m, 10 m, 15 m and 20 m, respectively. In other words, the dissipation of the pore water pressure in zone B at the depth of 5 m, 10 m, 15 m and 20 m was increased by 48%, 59%, 63% and 40%, respectively, in comparison to those in Zone A. Further, notable decreases were observed in the pore water pressure in Zone B after the activation of the booster system. With the aid of the booster system, the pore water pressure was further decreased by 10.7 kPa, 7.7 kPa, 5.1 kPa and 5 kPa at the depth of 5 m, 10 m, 15 m and 20 m, respectively. It is worth noting that the reduction in the pore water pressure was also apparent in the deep soil layer. For example, the pore water pressure dissipated in the last 20 days could account for 8.4% of the total dissipation of the pore water pressure at the depth of 20 m. It demonstrates that the improved air booster vacuum preloading technology is more effective for promoting the consolidation of the deep soil layer. For example, at the end of the test, the dissipation of pore water pressure in zone B at the depth of 5 m, 10 m, 15 m and 20 m was 58%, 66%, 67% and 44% larger than those in Zone A.

Fig. 9(c) shows the pore water pressure measured during boosting on the first day of the activation of the booster system. As can be seen, the pore water pressure fluctuated significantly during the pressurization. Finally, the pressurization caused notable reductions in the pore water pressures. For example, the pore water pressure was dropped by 1.4 kPa, 1.2 kPa, 0.8 kPa and 0.5 kPa at the depth of 5, 10, 15 and 20 m, respectively, at the end of the pressurization.

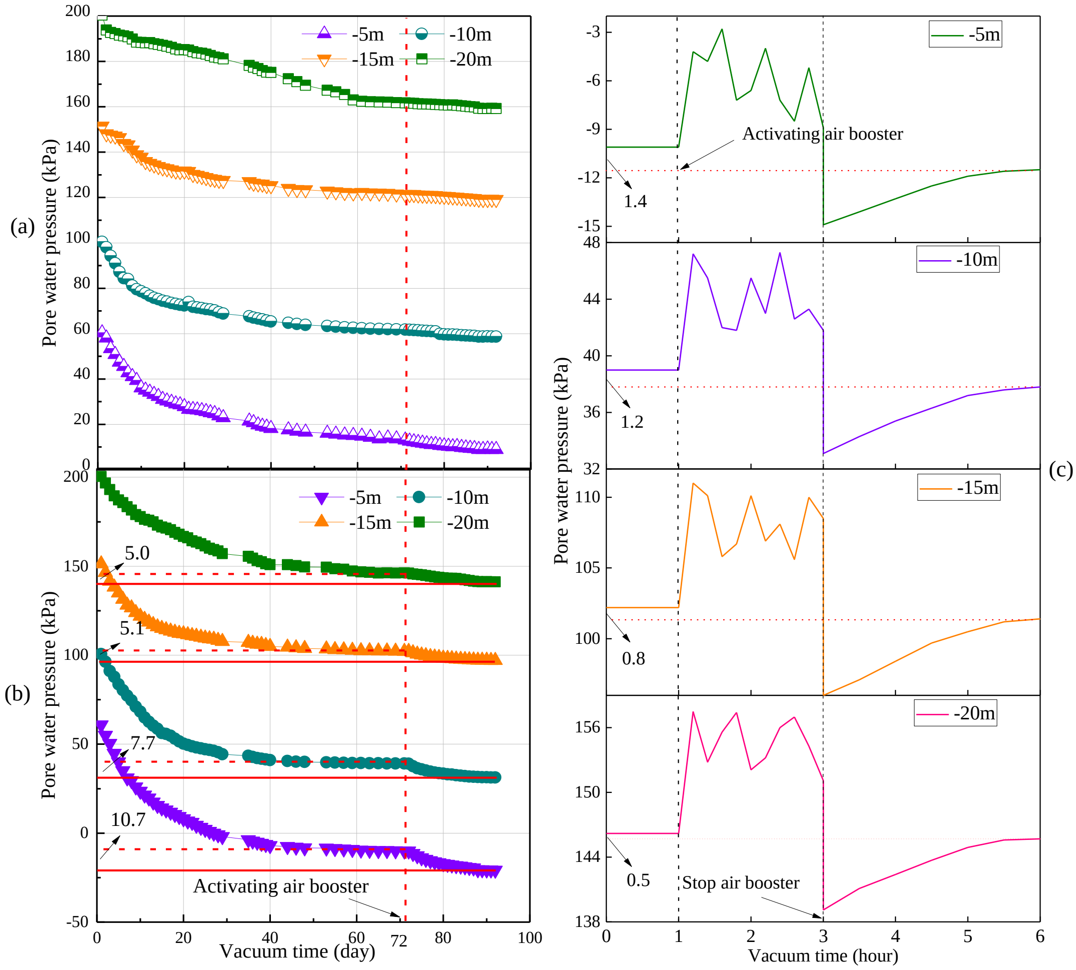

Fig. 9. Variations in the pore water pressure at different depths: (a) in zone A; (b) in zone B; (c) on the first day of the activation of the booster system in Zone B

4.3 Degree of consolidation

The average degree of consolidation (DOC) can be calculated from the monitored pore water pressure. The distribution profiles of the monitored pore water pressure are illustrated in Fig. 10, with which the average DOC, U_{avg}, can be calculated as follows:

$$U_{avg} = 1 - \frac{\int [u_t(z) - u_s(z)]dz}{\int [u_0(z) - u_s(z)]dz} \quad [3]$$

and

$$U_s(z) = \gamma_w z - s(kPa) \quad [4]$$

where $u_0(z)$ is the initial pore water pressure at depth z; $u_t(z)$ is the final pore water pressure at depth z; $u_s(z)$ is the suction at depth z; γ_w is the unit weight of water; and s is the applied suction (80 kPa). The integrals in the numerator and denominator of Eq. (4) can be calculated using the area between the curve $u_t(z)$ and the line $u_s(z)$. According to the formulation in Eq. (4), the U_{avg} can be calculated and the results are shown in Fig. 10, the calculated U_{avg} in Zone B was 80% and that in Zone A was 52%. DOC at different time is shown in Table 2. A comparison of the calculated DOC at the elapsed time of 72 days and 92 days indicates that the most contribution is associated with the airtight connection vacuum system. However, Table 2 shows that the increased of DOC in Zone B is greater than that in Zone A during the last 20 days. This table result also supports the statement that the improved air booster vacuum preloading technology accelerates the consolidation of the soil.

Table. 2. Degree of consolidation at different times in both zones

Time (days)	DOC (Zone A)	DOC (Zone B)
72	49%	74%
92	52%	80%

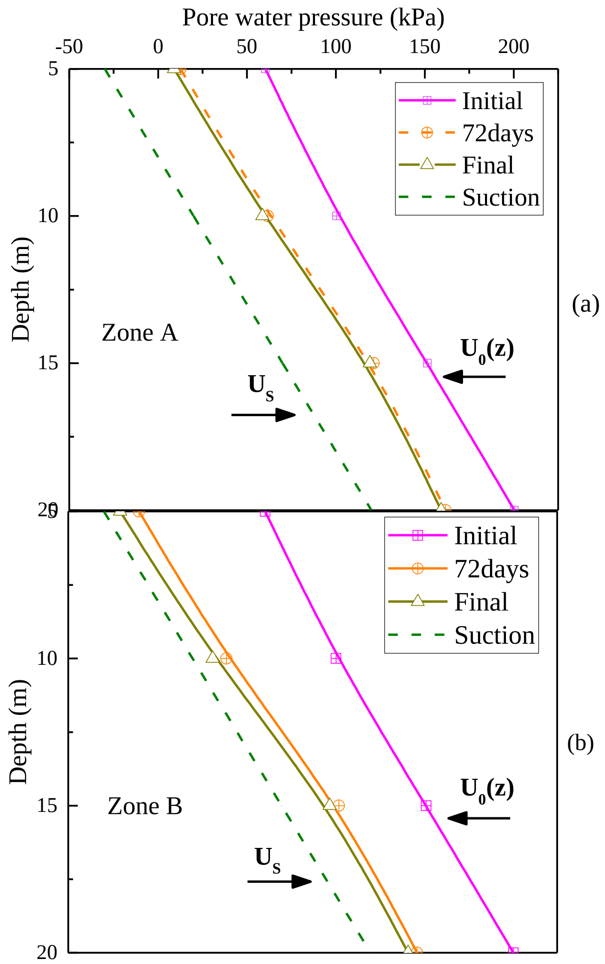

Fig. 10. Pore water pressure distribution with depth: (a) zone A and (b) zone B

4.4 Surface settlement

Fig. 11 presents the evolution of the ground surface settlement in the two zones. At the beginning of the preloading, the surface settlement in zone A was slightly larger than that in zone B. It is attributed to the fact that Zone A was subjected to an additional surcharge which was applied by the 0.5 m thick sand blanket on the ground surface. After the 15 days' preloading, the surface settlement in Zone B, however, began to exceed that in Zone A. As the preloading proceeded, the increase in the surface settlement slowed down in both zones. At the end of 72 days' preloading, the difference between the average surface settlements in the two zones was as large as

212.5 mm. Thus, the faster consolidation of the soil was achieved by the improved air booster vacuum preloading technology. The surface settlement in Zone B tended to converge before the activation of the booster system, whereas the surface settlement in zone A did not converge until 85 days. When the booster system in Zone B was activated, notable increment in the surface settlement occurred. During the boosting period, the average surface settlement in Zone B was increased by 103.5 mm, which accounted for 6% of the total surface settlement; in contrast, the average total surface settlement in Zone A was only increased by 46.5 mm only, accounting for 3% of the total surface settlement. In other words, the surface settlement accumulated in this period in Zone B was two times of that in Zone A; and, part of the settlement difference in the two zones is due to the air-boosting. Thus, the improved air booster vacuum preloading technology helps accelerate the consolidation of soil. At the end of the test, the average surface settlement in zone A and zone B was 1457 mm and 1722.5 mm, respectively.

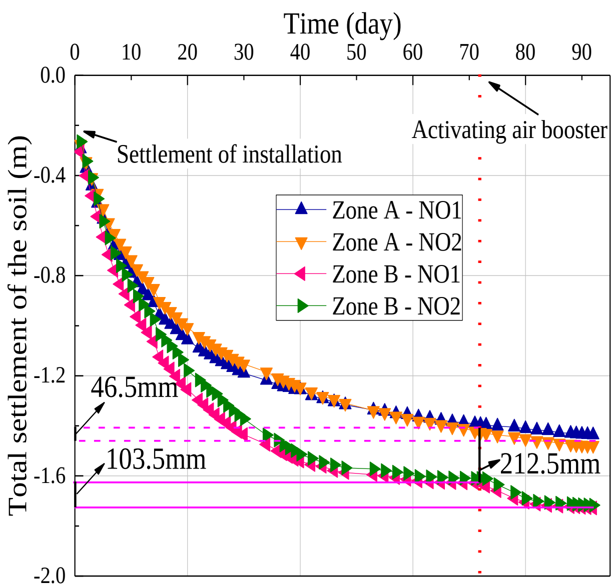

Fig. 11. Monitored total surface settlements against elapsed time for the two zones

4.5 Layered settlement

Fig. 12 plots the evolution of layered settlement in the two zones. In zone A, the layered settlement increased with decreasing of growth rate as the test proceeded, as shown in Fig. 12(a). In zone B, the evolution of the layered settlement was similar to that in Zone A before the activation of the booster system, as shown in Fig. 12(b). However, the accumulated settlement in zone B was larger than that in zone A, which can be attributed to the airtight connections adopted in the improved air booster vacuum preloading technology. After the activation of the booster system, obvious increment in the layered settlement was found in Zone B. During the last 20 days, the accumulated settlement in Zone B was 86 mm, 80 mm, 20 mm, 12 mm and 5 mm at the depth of 2 m, 4m, 16 m, 18 m and 20 m, respectively; whereas, in the same period, the accumulated settlement in Zone A was only 43 mm, 39 mm, 9 mm, 5 mm and 2 mm at the depth of 2 m, 4m, 16 m, 18 m and 20 m, respectively. As can be seen, the accumulated settlement in Zone B during the last 20 days has a significant increase at each layer with the help of a booster system. Thus, the improved air booster vacuum preloading technology is more competent for improving the deep marine clay layers.

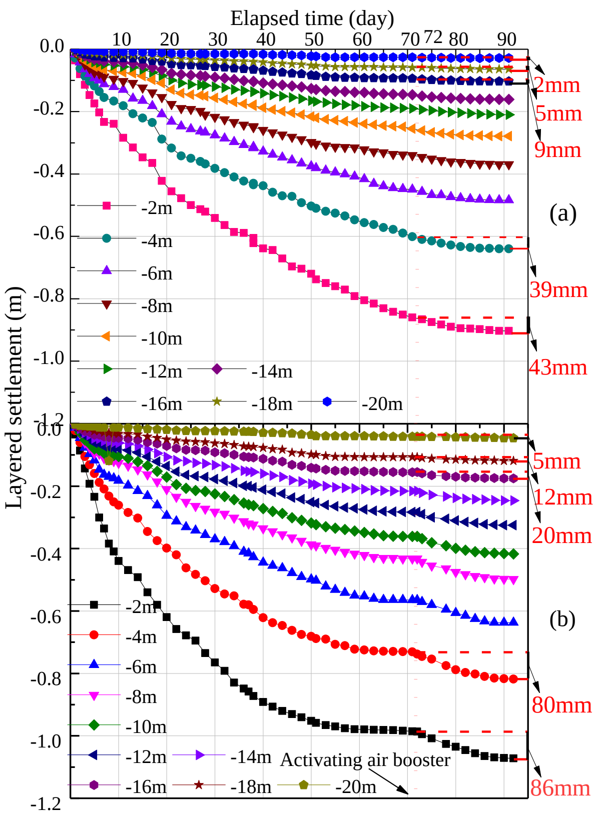

Fig. 12. Layered settlements measured at different depths during vacuum preloading against elapsed time: (a) Zone A and (b) Zone B

4.6 Lateral displacement

It is known that a vacuum pressure tends to induce inward displacement (toward the center of a zone) in the soil, and Fig. 13 presents the profile of the lateral displacement in the two zones. The plots in Figure 13 indicated the lateral displacements in the two zones were similar. The lateral displacement gradually decreased with the depth; however, the lateral displacement in zone A was smaller than that in zone B, especially in the shallow soil layer. For a deep analysis of the difference in the lateral displacement between these two zones, the lateral displacement is normalized herein by the maximum lateral displacement. In Fig. 14, the normalized lateral displacement at 20 days in Zone B is greater than that in Zone. At the end of 72 days' preloading, the lateral displacement at the ground surface in Zone B was 675 mm, which was 49% larger than that in zone A (i.e., 452 mm). When the booster system was activated, the lateral displacement at the ground surface in zone B was increased by 82 mm, while it was only increased by 13 mm in zone A; and, at the end of the test, the lateral displacement in zone A and zone B was 465 mm and 758 mm, respectively. Test results indicated that air booster vacuum preloading method can cause more lateral displacement, and the more lateral displacement means that the soil can get better compression and consolidation, which are more conducive to the later stage of engineering construction.

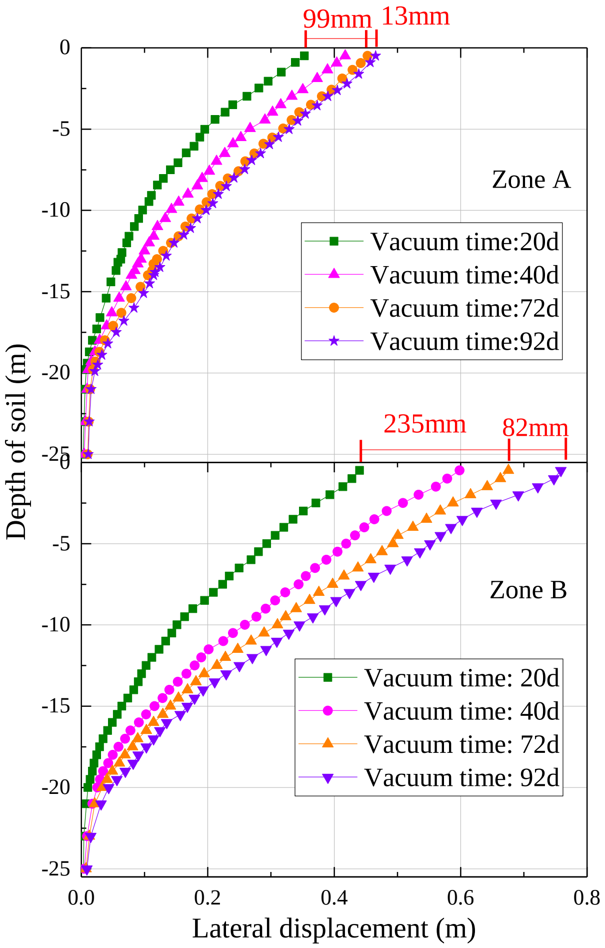

Fig. 13. Curves of the monitored lateral displacement against elapsed time

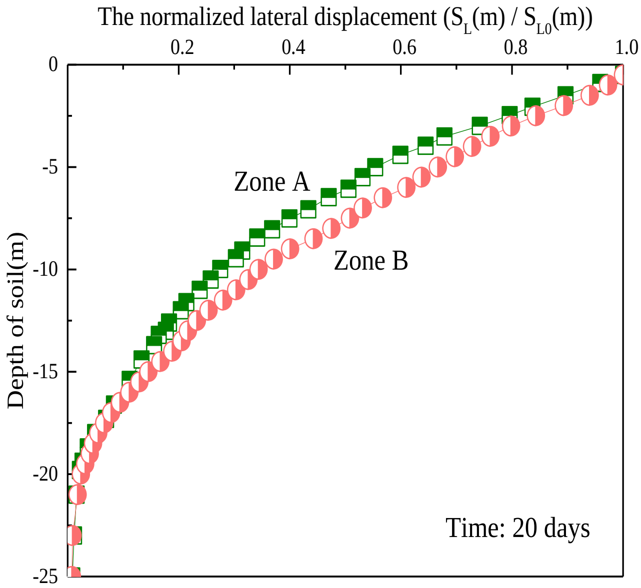

Fig. 14. Curves of the normalized lateral displacement against elapsed time in two zones at 20 days

4.7 Water content

Fig. 15 shows the water content profiles in the two zones. Before the preloading, the water content was more than 45% within the depth of 20 m, and which was 65% in the shallow soil layer. After the ground treatment, significant reductions in the water content were observed in both zones. For example, the water content in the shallow soil layer was reduced to 38.8% and 34.3% in zone A and Zone B, respectively. Further, the water content profiles in the two zones were similar in shape and it generally increased with the depth; however, at a given depth, the water content in Zone B tended to be smaller than that in Zone A. Here, the average water content in the deep soil layer (i.e., 15 m~20 m) in zone B was reduced by 10% while that in Zone A was only reduced by 4%. Thus, the improved air booster vacuum preloading technology outperformed the conventional vacuum preloading technology in the soft soil improvement.

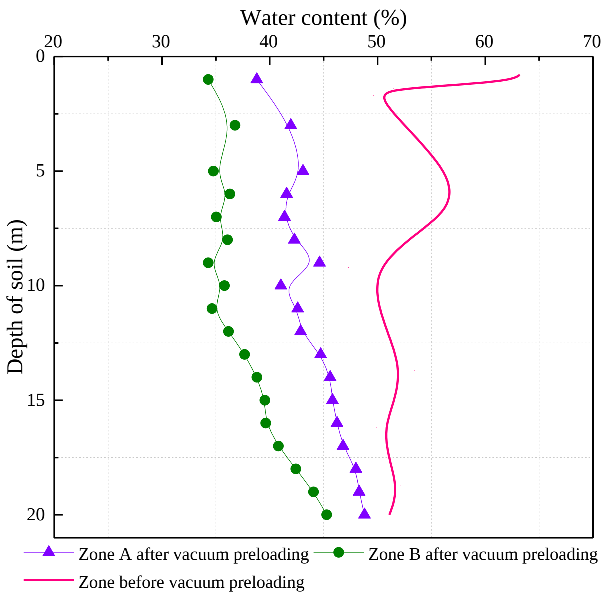

Fig. 15. Measured water content profiles in the initial and final stage

4.8 Vane shear strength

Fig. 16 presents the shear strength profiles in the two zones which are obtained with the vane shear tests. Before the ground improvement, the vane shear strength was less than 25 kPa within the depth of 20 m, and the vane shear strength was as small as 15 kPa in the shallow soil layer. After the ground improvement, the vane shear strength in both zones increased significantly. For instance, the vane shear strength in the shallow soil layer was increased to 37.8 kPa and 43.2 kPa in Zone A and Zone B, respectively. The profiles of the vane shear strength in both zones showed the same behavior. In both zones, the shear strength decreases as the depth increases in a general trend. Further, the vane shear strength in Zone B was always larger than that in Zone A. Here, notable increment in the vane shear strength in the deep soil layer was also achieved by the improved air booster vacuum preloading technology. For example, the vane shear strength at the depth of 20 m was increased from 23.9 kPa to 32.0 kPa in Zone B, while it was only increased to 27.1 kPa in Zone A. Thus, the superiority of the improved air booster vacuum preloading technology was demonstrated.

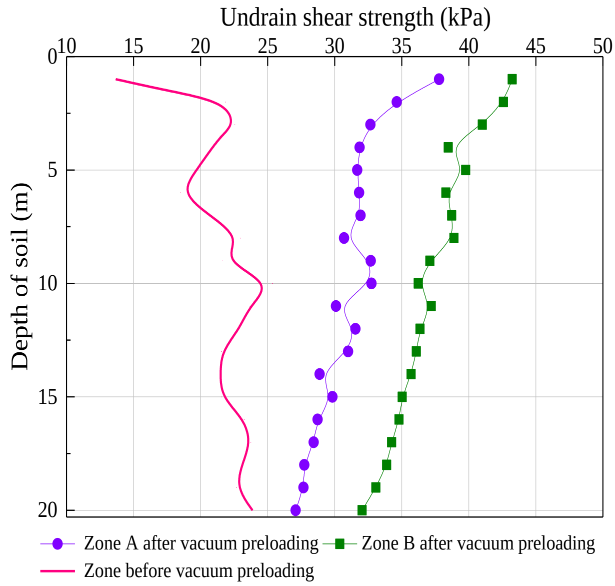

Fig. 16. Measured field vane shear strength profiles in the initial and final stage

4.9 Cone resistance and sleeve friction

Fig. 17 shows the cone resistance and frictional resistance in the two zones obtained with the cone penetration tests. For better analysis of soil reinforcement at different depths, the soil was divided into four segments along the depth, and the average cone resistance and fictional resistance was calculated for each segment. Before the ground improvement, both cone resistance and sleeve friction resistance were small. Within the depth of 20 m, the cone resistance was smaller than 0.21 MPa and the sleeve friction was smaller than 8.1 kPa. After the ground improvement, both cone resistance and sleeve friction gained significant increases. For example, the average cone resistance in Segment IV was increased from 0.11 MPa to 0.43 MPa in Zone A and 0.53 MPa in Zone B; and, the average sleeve friction in Segment IV was increased from 4.4 kPa to 11.8 kPa in Zone A and 14.8 kPa in Zone B. That is to say, both cone resistance and sleeve friction in zone B were larger than those in zone A. The average cone resistance in the four segments in Zone B was 55%, 39%, 30% and 23% larger than that in Zone A, and the average sleeve friction in the four segments in Zone B were 67%, 26%, 43% and 25% larger than that in Zone A. Thus the developed air booster vacuum preloading technology was more effective that the conventional vacuum preloading technology.

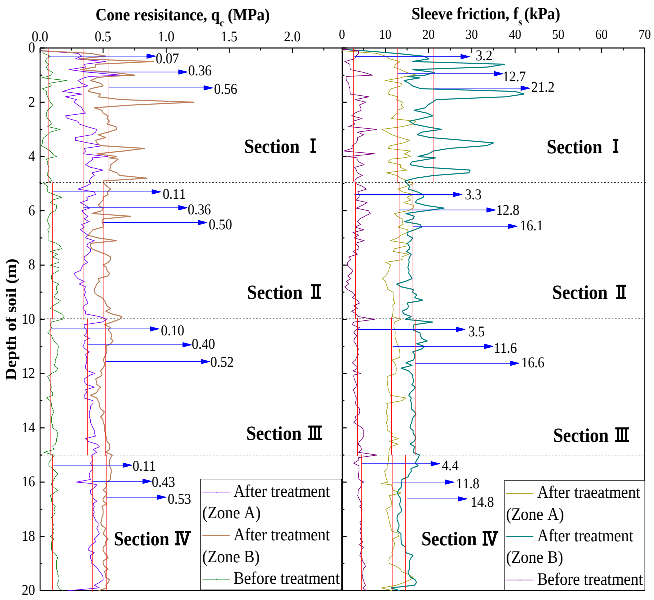

Fig. 17. Measured frictional resistance and cone resistance profiles in the initial and final stage

5 Conclusions

This study proposed an improved air booster vacuum preloading technology for the ground improvement of deep marine clay layers, in which the conventional booster tube was replaced by the booster PVD. In-situ field tests were conducted at Oufei sluice project to examine the performance of the improved air booster vacuum preloading technology. A comprehensive monitoring system was implemented to measure the vacuum pressure, pore water pressure, settlement, and lateral displacement.

The analysis of the monitoring data was carried out to evaluate the extent of soil improvement. The major conclusions of this study are as follows:

(1) The improved air booster vacuum preloading technology is shown superior to the conventional vacuum preloading technology. For the conventional vacuum preloading, the dissipation of the pore water pressure almost vanished after 72 days within 20m depths. For the air booster vacuum preloading, notable reductions appeared in the pore water pressures after the activation of the booster system, and the pore water pressure dissipation in the deep soil layer was particularly apparent.

(2) The improved air booster vacuum preloading technology performs better than the conventional vacuum preloading technology. During last 20 days, the layered settlement generated by the former was more than double the counterpart yielded by the latter.

(3) The improved air booster vacuum preloading technology is more competent than the conventional vacuum preloading technology in improving the physical and mechanical properties of the soil. The vane shear strength of the soil enhanced by the former was always larger than its counterpart improved by the latter. Both cone resistance and frictional resistance of the soil achieved by the former were larger than their counterparts by the latter.

Acknowledgements

This research was supported by National Key R&D Program of China (2016YFC0800200）, the Program of International Science and Technology Cooperation (No. 2015DFA71550), the National Natural Science Foundation of China

(No. 51622810, No. 51778501 and No. 51620105008), the Zhejiang Province Natural Science Foundation of China under Grant No. LR18E080001, and the Key Research and Development Program of Zhejiang Province under Grant No. 2018C03038. This financial support is gratefully acknowledged.

Notation

Basic SI units are shown in parentheses

W_L Liquid limit (dimensionless)

W_P Plastic limit (dimensionless)

W Water content (dimensionless)

G_S Specific gravity (dimensionless)

e_0 Void ratio (dimensionless)

C_u Undrained shear strength (Pa)

References

Azari, B., Fatahi, B., & Khabbaz, H. 2016. Assessment of the elastic-viscoplastic behavior of soft soils improved with vertical drains capturing reduced shear strength of a disturbed zone. International Journal of Geomechanics, 16(1), B4014001-15.

Bo, M.W. 2004. Discharge capacity of prefabricated vertical drain and their field measurements. Geotextiles & Geomembranes, **22**(1–2), 37-48.

Biot, M.A. 1941. General theory of three - dimensional consolidation. J.appl.phys, **12**(2), 155-164.

Chu, J., Yan, S. W., & Yang, H. 2000. Soil improvement by the vacuum preloading method for an oil storage station. Geotechnique, **50**(6), 625-632.

Chu, J., Bo, M.W., & Choa, V. 2004. Practical considerations for using vertical drains in soil improvement projects. Geotextiles & Geomembranes, **22**(1–2), 101-117.

Chu, J., and Yan, S.W. 2005a. Application of the vacuum preloading method in soil improvement projects. In Ground Improvement - Case Histories. Edited by I. Buddhima and C. Jian. Elsevier. pp. 91-117.

Chu, J., & Yan, S.W. 2005b. Estimation of degree of consolidation for vacuum preloading projects. International Journal of Geomechanics, **5**(2), 158-165.

Chu, J., & Yan, S.W. 2006. Effective depth of vacuum preloading. Lowland Technology International the Official Journal of the International Association of Lowland Technology, 8, 1-8.

Chai, J. C., & Miura, N. 1999. Investigation of factors affecting vertical drain behavior. Journal of Geotechnical & Geoenvironmental Engineering, **125**(3), 216-226.

Chai, J. C., Miura, N., & Nomura, T. 2004. Effect of hydraulic radius on long-term drainage capacity of geosynthetics drains. Geotextiles & Geomembranes, **22**(1), 3-16.

Chai, J.C., Carter, J.P., & Hayashi, S. 2005. Ground deformation induced by vacuum consolidation. Journal of Geotechnical & Geoenvironmental Engineering, **131**(12), 1552-1561.

Chai, J.C., Carter, J.P., & Hayashi, S. 2006. Vacuum consolidation and its combination with embankment loading. Canadian Geotechnical Journal, **43**(10), 985-996.

Chai, J.C., Hong, Z. & Shen, S. 2010. Vacuum-drain consolidation induced pressure distribution and ground deformation. Geotextiles and Geomembranes, 28, No. 6, 525–535.

Chai, J.C., & Carter, J.P. 2011. Deformation Analysis in Soft Ground Improvement. Springer Netherlands.

Cai, Y., Qiao, H., Wang, J., Geng, X., Wang, P., Cai, Y., 2017. Experimental tests on effect of deformed prefabricated vertical drains in dredged soil on consolidation via vacuum preloading. Engineering Geology 222, 10-19.

Ding, H.L., Guo, Z.P., Fan, K.Y., Wang, Z.T.,&Qian, M. 2015. Comparative Experiment aon Soft Soil Treatment by Air-boostedVacuum Preloading. Chinese Journal of Underground Space and Engineering. 11(S1): 1673-0836(in Chinese).

Fu, H.T., Cai, Y.Q., Wang*, J., Wang, P. 2017. Experimental study on the combined application of vacuum preloading-variable-spacing electro-osmosis to soft ground improvement. Geosynthetics International . 24(1): 72-81.

Fu, H.T., Fang, Z.Q., Wang*, J., Chai, J.C., Cai, Y.Q., Geng, X.Y., Jin, J.Q. & Jin, F.Y. 2018. Experimental Comparison of Electro-Osmotic Consolidation of Wenzhou Dredged Clay Sediment Using Intermittent Current and Polarity Reversal. Marine Georesources & Geotechnology. 36(1):131-138.

Haeri, S. M., Khosravi, A., Garakani, A. A., & Ghazizadeh, S. 2016. Effect of soil structure and disturbance on hydromechanical behavior of collapsible loessial soils. International Journal of Geomechanics, 17(1), 04016021.

Han, W. J., Liu, S. Y., Zhang, D. W., & Du, G. (2012). Field Behavior of Jet Grouting

Pile under Vacuum Preloading of Soft Soils with Deep Sand Layer. Geocongress (pp.70-77).

Indraratna, B., Rujikiatkamjorn, C., & Balasubramaniam, A.S. 2014. Consolidation of estuarine marine clays for coastal reclamation using vacuum and surcharge loading. Geotechnical Special Publication(233), 358-369.

Kjellman, W. 1952. Consolidation of clayey soils by atmospheric pressure. Proceedings of a Conference on Soil Stabilization, Massachusetts Institute of Technology, USA: 258-263.

Kianfar, K., Indraratna, B., Rujikiatkamjorn, C., & Leroueil, S. 2015. Radial consolidation response upon the application and removal of vacuum and fill loading. Canadian Geotechnical Journal, 52(12): 2156-2162

Liu, H., Yu, X.P., et al. 2014. Comparative experiment study on the strengthening of dredger fill using vacuum preloading method based on pressurization and anti-clogging technology [J]. Railway standard design, **58**(1): 28-33 (in Chinese)

Liu, F.Y., Fu, H.T., Wang*, J., Mi, W. 2017. Influence of soluble salt on electro-osmotic consolidation of soft clay. Soil Mechanics and Foundation Engineering. 54(1):49-55

Li, A. G., Tham, L. G., Wen, J. P., & Chen, S. C. (2014). Case study of ground improvement to qianhai reclamation area, qianhai bay, shenzhen. Geotechnical Special Publication(238), 231-240.

Li, B., Wu, S. F., Chu, J., & Lam, K. P. (2011). Evaluation of Two Vacuum Preloading. Techniques Using Model Tests. Geo-Frontiers Congress (pp.636-645).

Onoue, A. 1988. Consolidation by vertical drains taking well resistance and smear into consideration. Soils & Foundations, **28**(4), 165-174.

Perera, D., Indraratna, B., Leroueil, S., Rujikiatkamjorn, C., & Kelly, R. 2016. An analytical model for vacuum consolidation incorporating soil disturbance caused by mandrel-driven drains. Canadian Geotechnical Journal.54(4) : 547-560
DOI: 10.1139/cgj-2016-0232

Rixner, J.J., Kraemer, S.R., & Smith, A.D. 1986. Prefabricated vertical drains. volume 2. summary of research effort. Facilities.

Saowapakpiboon, J., Bergado, D.T., Chai, J.C., Kovittayanon, N., & Zwart, T.P.D. 2008. Vacuum-PVD Combination with Embankment Loading Consolidation in Soft Bangkok Clay: A Case Study of the Suvarnabhumi Airport Project. Geosynthetics in Civil and Environmental Engineering. Springer Berlin Heidelberg.

Shen, S.L, Chai, J.C., Hong, Z-S., and Cai, F.X. 2005. Analysis of field performance of embankments on soft clay deposit with and without PVD-improvement, Geotextiles and Geomemberanes, 23(6), 463-485.

Shen, Y.P., Yu, J., Liu, H., & Li, Z. 2011. Experiment study on air-boosted vacuum preloading of soft station foundation [J]. Journal of the China Railway Society, **33** (5): 97-103. (in Chinese)

Shen, Y.P., Feng, R.L., Zhong, S.Y., & Li, Z. 2012. Study on optimized design of vacuum preloading with air pressure boosted for treatment of railway station &

yard foundation [J]. Journal of the China railway society, **34** (4): 88-93. (in Chinese)

Shen, Y., Wang, H., Tian, Y., Feng, R., Liu, J., & Wu, L. 2015. A new approach to improve soft ground in a railway station applying air-boosted vacuum preloading. Geotechnical Testing Journal, **38**(4).

Sun, L., Guo, W., Chu, J., Nie, W., Ren, Y., & Yan, S., et al. 2017. A pilot test on a membraneless vacuum preloading method. Geotextiles & Geomembranes.

Wang, J., Cai, Y., Ma, J., Chu, J., Fu, H., & Wang, P., et al. 2016a. Improved vacuum preloading method for consolidation of dredged clay-slurry fill. Journal of Geotechnical & Geoenvironmental Engineering, ASCE, 142(11), 06016012.

Wang, J., Ma, J., Liu, F. 2016b. Experimental study on the improvement of marine clay slurry by electroosmosis-vacuum preloading. Geotextiles and Geomembranes. 44:615－622.

Wang, J., Ni, J., Cai, Y., Fu, H., and Wang, P. 2017. Combination of vacuum preloading and lime treatment for improvement of dredged fill. Engineering Geology, 227, 149-158.

Wang J, Fu, H.T., Liu, F.Y., Cai, Y.Q., & Zhou, J. 2018a. Influence of the electro-osmosis activation time on vacuum electro-osmosis consolidation of a dredged slurry. Canadian Geotechnical Journal. 55(1):147-153.

Wang, J., Cai, Y., Ni, J., Geng, X., and Xu, F. 2018b. "Effect of sand on the vacuum consolidation of dredged slurry." Marine Georesources & Geotechnology, 36(02), 238-244.

Wu, H.N., Shen, S.L., Ma, L., Yin, Z.Y., and Horpibulsuk, S. 2015. Evaluation of the strength increase of marine clay under staged embankment loading: a case study, Marine Georesources and Geotechnology, 33(6), 532-541.

Yoshikuni, H., & Nakanodo, H. 1974. Consolidation of soils by vertical drain wells with finite hydraulic conductivity. Soil Found, **14**(2), 35-46.

Yu, X. J., & Shi, J. Y. 2009. Research on the Disturbed State Concept for Soft Clay Roadbed. Geohunan International Conference (pp.92-98).